Proceedings of ICRC 2001: 1956 © Copernicus Gesellschaft 2001

ICRC 2001

New measurements of fragmentation cross sections from ^{56}Fe and ^{60}Ni beams at energies relevant to galactic cosmic-ray propagation

J. S. George[1], R. A. Mewaldt[1], N. E. Yanasak[1], M. E. Wiedenbeck[2], J. J. Connell[3], L. Audouin[4], C.-O. Bacri[4], B. Berthier[4], L. Ferrant[4], F. Rejmund[4], C. Stephan[4], L. Tassan-Got[4], D. Karamanis[5], S. Czajkowski[5], A. Boudard[6], J.-E. Ducret[6], B. Fernandez[6], S. Leray[6], C. Villagrasa[6], C. Volant[6], T. Faestermann[7], T. Enqvist[8], F. Hammache[8], K. Helariutta[8], B. Jurado[8], K. H. Schmidt[8], K. Sümmerer[8], M. V. Ricciardi[8], F. Vivès[8], A. Heinz[9], J. Benlliure[10], E. Casarejos[10], M. F. Ordoñez[10], J. Pereira-Conca[10], and A. R. Junghans[11]

[1]California Institute of Technology, Pasadena, CA 91125 USA
[2]Jet Propulsion Laboratory, California Institute of Technology, Pasadena, CA 91109 USA
[3]University of Chicago, Chicago, IL 60637 USA
[4]Institut de Physique Nucléaire, 91406 Orsay cedex, France
[5]CEN-Bordeaux Gradignan, F33175 Bordeaux, France
[6]DAPNIA/SPhN, CEA/Saclay, 91191 Gif-sur-Yvette cedex, France
[7]TU Muenchen, 85747 Garching, Germany
[8]GSI, Planckstrasse 1, D-64291 Darmstadt, Germany
[9]Argonne National Laboratory, Argonne, IL 60439-4083, USA
[10]Universidad de Santiago de Compostela, 15706 Santiago de Compostela, Spain
[11]CENPA/University of Washington, Seattle WA 98195 USA

Abstract. Models of cosmic-ray propagation in the Galaxy rely heavily on knowledge of the nuclear fragmentation cross sections which govern spallation of heavy nuclei in the interstellar medium. Interpretation of high-precision cosmic-ray composition data such as those from the ACE and Ulysses missions requires improved cross-section data. New measurements of partial fragmentation cross sections have been made with high statistical accuracy at the GSI heavy ion synchrotron (SIS) using ^{56}Fe beams at five energies between 300 and 1500 MeV/nucleon, and ^{60}Ni beams at 500 and 1000 MeV/nucleon, on a liquid hydrogen target. We report on progress in analyzing these data.

1 Introduction

Cosmic-ray propagation models describe the processes that affect the composition of energetic nuclei during transport through the Galaxy from their source to the Earth. Spallation of ^{56}Fe on the H and He in the interstellar medium (ISM) accounts for most of the observed Sc-Mn abundance in galactic cosmic rays and makes significant contributions to the secondary components of elements well below Ca. The sub-Fe elemental abundances constrain the amount of matter traversed by the cosmic rays. Specific nuclides probe the confinement time in the Galaxy and the possibility of acceleration by multiple shocks. Isotopes just beyond ^{56}Fe have significant primary contributions and are important probes of stellar nucleosynthesis and the time delay between production and acceleration (Wiedenbeck et al., 1999). Spallation contributions to these isotopes come predominately from ^{60}Ni, for which partial fragmentation cross sections have never been measured.

Correspondence to: J. S. George (george@srl.caltech.edu)

The combined high-precision cosmic-ray data from the Advanced Composition Explorer (ACE) and Ulysses spacecraft are no longer limited by statistics. Instead, uncertainties in the propagation model parameters, particularly in the nuclear fragmentation cross sections, restrict the interpretation of the data. The availability of measurements with good statistical accuracy in multiple energy bins also means that the energy dependence of the cross sections is now of even greater importance. Semi-empirical formulae used to estimate the cross sections are often not well constrained by the available measurements and lead to large differences in predictions for secondary production.

Recently (October 2000), our team of researchers from Europe and the USA made new measurements of partial fragmentation cross sections for ^{56}Fe and ^{60}Ni on a hydrogen target. These measurements are important not only for astrophysical applications, but also for the design of accelerator-driven systems (ADS) which could be a potential solution to the problems of nuclear energy production and nuclear waste transmutation (Bowman et al., 1992). To this end the experiment included measurements using a deuterium target. We focus here on the sub-Fe fragments ($Z \leq 20$) from spallation of ^{56}Fe and ^{60}Ni that are most relevant for cosmic-ray models.

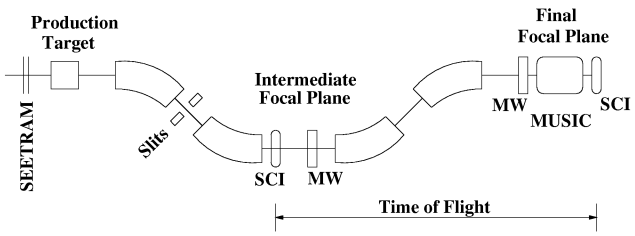

Fig. 1. Schematic layout of the FRS fragment spectrometer. Fragments are separated by the four large dipole magnets. Scintillators (SCI) measure the time of flight over the second half of the spectrometer as well as the horizontal beam position. Multi-wire chambers (MW) are used for beam tuning and removed for production measurements.

2 The Experiment

The new measurements were made at the GSI heavy ion synchrotron (SIS) located in Darmstadt, Germany. Beams of ^{56}Fe and ^{60}Ni were accelerated to energies of 0.3, 0.5, 0.75, 1.0, and 1.5 GeV/nucleon, and 0.5 and 1.0 GeV/nucleon, respectively. The primary beam intensity was monitored using a secondary electron transmission monitor (SEETRAM), cross-calibrated at low count rates with a plastic scintillator. The primary beams were extracted from the synchrotron and directed onto a liquid hydrogen production target (Golovanov, 1996). Measurements were repeated in subsequent runs using an identical empty target to allow subtraction of contributions to fragment production by structures in the target and beam line.

Fragments produced in the target were separated with the FRS fragment separator operated as an achromatic magnetic spectrometer (Geissel et al., 1992). Figure 1 is a schematic diagram of the FRS showing the four large dipole magnets used to select the fragments. Partial transmission of fragments with rigidities close to those of the primary nuclei was accomplished by inserting slits from either side to block the remaining beam after the target.

The mass-to-charge ratio, A/Z, of the fragments was determined from the magnetic rigidity using the relation

$$\frac{A}{Z} = \frac{eB\rho}{cm_u\beta\gamma} \quad (1)$$

where c is the speed of light, e is the elementary charge, and m_u is the atomic mass unit. The dipole magnetic fields B for each setting were measured with Hall probes and the effective radius of curvature ρ was determined using a reference beam of primary nuclei. Corrections for position at the final focal plane, measured with a plastic scintillator, were applied to improve the resolution. The velocity β, and Lorentz factor γ, were determined by a time-of-flight measurement using scintillators at the intermediate and final focal planes. Because the FRS has a momentum acceptance of $\pm$1.6%, full coverage of the desired fragments required as many as 18 overlapping settings.

The nuclear charge, Z, was determined using a multiple sampling ionization chamber (MUSIC) (Pfützner, 1994).

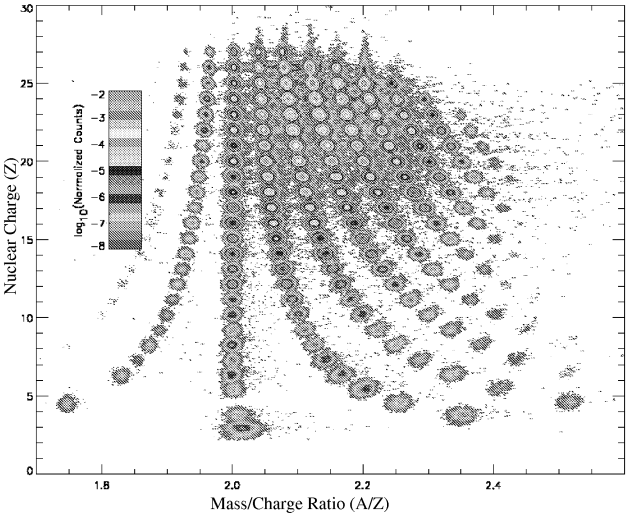

Fig. 2. Complete isotope coverage in Z vs. A/Z for 500 MeV/nucleon ^{56}Fe beam on a ^{1}H target. Plot is made by superimposing data from overlapping magnet settings, normalized to the primary beam intensity.

Energy loss in the gas produced a signal proportional to Z^2/β^2, allowing a determination of Z with a resolution of 0.15 charge units. Relative timing between the anode signals in MUSIC provided a measurement of the horizontal angle at which the fragments entered the detector.

Figure 2 shows the complete fragment coverage in Z vs. A/Z for 500 MeV/nucleon ^{56}Fe on the hydrogen target. The plot was made by adding histograms from individual settings, each normalized to the intensity of the primary beam. The fragments are well resolved and easily identifiable down to boron (Z=5). Nearly all isotopes from Ca to Fe have statistical uncertainties well below 1% with as many as 8x10^5 particles contributing to a single spot. This easily surpasses the scientific goal of a 5% measurement precision for the major isotopes. The final precision will be determined by the systematic uncertainties in the normalization to the primary beam intensity and other corrections. A few of the rarest nuclides at the extreme edges of the coverage have statistical uncertainties $\sim$6-10%.

The preliminary nature of this work is seen in artifacts remaining in Figure 2 such as a very low background between the high-intensity isotope spots. Vertical bands extending upward from the heaviest nuclei indicate chance coincidences of multiple particles in MUSIC. These issues are being addressed and will be resolved in the final analysis. In practice, the isotope selection is made with a small ellipse centered on each spot so extraneous events between spots do not significantly contribute to the calculated yields.

Once the mass and charge are identified using the energy loss in MUSIC and the time-of-flight measurement, the distribution of $\beta\gamma$ values is reconstructed using the magnet settings in the first half of the FRS. Isotopes which are incompletely transmitted in a single setting will contribute a slice of the full fragment distribution with the missing pieces being

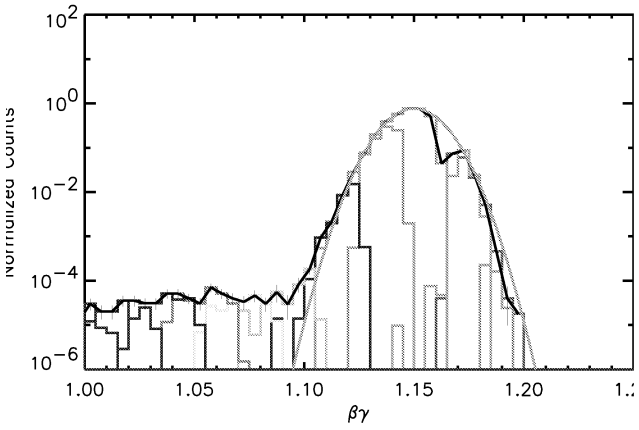

Fig. 3. Full $\beta\gamma$ distribution for ^{45}Sc fragments produced from 500 MeV/nucleon ^{56}Fe on a hydrogen target. Each histogram corresponds to a slice of the full distribution measured in a single magnet setting. The dark line follows the envelope of the superimposed histograms and the light curve is a Gaussian fit. The deficit around $\beta\gamma$=1.16 comes from incomplete transmission due to the slits used to block the primary beam.

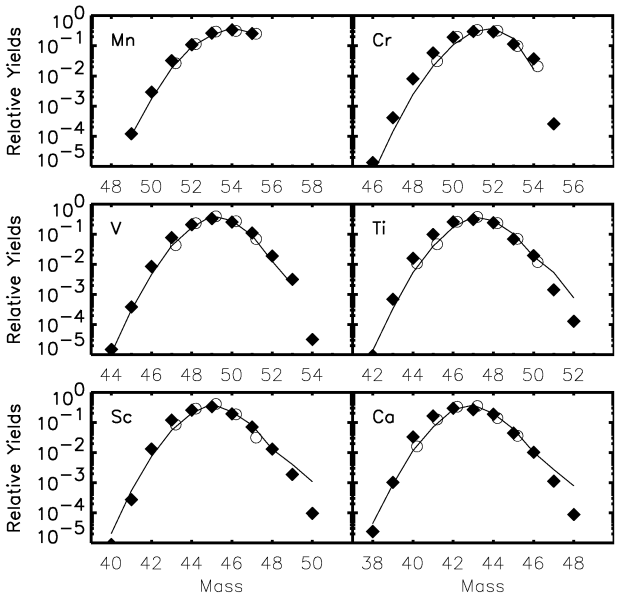

Fig. 4. Fractional yields from a 500 MeV/nucleon ^{56}Fe primary beam on a hydrogen target. The dark diamonds are the current preliminary results, open circles represent data from Webber et al. (1998). The solid line gives predictions from the Silberberg and Tsao semi-empirical formulae. Each data set and the predictions are separately normalized to the total yield for each element.

recovered in neighboring settings. Figure 3 shows how the superimposed $\beta\gamma$ histograms for ^{45}Sc fragments, each normalized to the beam intensity, combine to map out the full distribution. The heavy dark line follows the envelope of the overlaid histograms and the light curve is a Gaussian fit. A low-momentum tail on the left side of the distribution occurs only for abundant fragments and is more than four orders of magnitude below the peak.

An advantage of fitting the $\beta\gamma$ distribution to derive the reaction yield is that transmission losses near the edge of the angular acceptance are mitigated by contributions from overlapping settings. Gaps in the momentum coverage, such as where slits blocked the primary beam, are easily corrected by fitting the rest of the distribution. The area under each curve is proportional to the partial cross section.

3 Discussion

Figure 4 shows relative yields for sub-Fe isotopes from a 500 MeV/nucleon ^{56}Fe beam on a liquid hydrogen target normalized to the total yield for each element. The solid line represents the prediction of the Silberberg & Tsao semi-empirical formulae at 500 MeV/nucleon, similarly normalized (Silberberg et al., 1998; Tsao et al., 1998). Data from Webber et al. (1998) at 576 MeV/nucleon are plotted as open circles, slightly offset to the right for clarity. The Webber data were clearly used to constrain the semi-empirical predictions.

The preliminary yields shown here are in qualitative agreement with the Webber measurements. We find higher yields for lighter isotopes and for isotopes at the extremes of the previous fragment coverage. The semi-empirical formulae follow the Webber data where available, but show marked deviations from our yields for the heaviest fragments.

When completed, these new cross-section measurements will be immediately applicable to a number of important questions related to cosmic-ray astrophysics. In particular, the abundance of ^{48}Ca offers a probe into the nucleosynthetic origins of the source material (Wiedenbeck et al., 2001b). Even though ^{48}Ca is extremely rare in the cosmic rays, it is difficult to produce by fragmentation of ^{56}Fe. This implies that most of the observed ^{48}Ca comes directly from the source. Our preliminary yields for ^{48}Ca from ^{56}Fe fragmentation relative to the total Ca yield are a factor of ∼5-10 lower than the semi-empirical predictions with ∼250 particles contributing from the 500 MeV/nucleon ^{56}Fe runs. Similar results have been obtained from the 1 GeV/nucleon runs. The momentum distributions for the Ca isotopes have essentially no background and there is no indication that the low yield is attributable to transmission losses or fitting errors. The implication is that the observed ^{48}Ca cosmic-ray abundance is of a substantially primary origin.

Radioactive isotopes such as ^{49}V and ^{51}Cr produced during cosmic-ray transport through the Galaxy show evidence of decay due to electron-capture at low energies. This decay happens only at energies low enough for the stripped ions to attach an electron from the interstellar medium (Connell and Simpson, 1999; Niebur et al., 2001). If the cosmic rays were accelerated incrementally by multiple shocks over a period of time, the effects of decay during the lower energy stages would be observed at Earth in the parent/daughter ratios at higher energies. The interpretation of new high-precision measurements of these isotopes from ACE is presently lim-

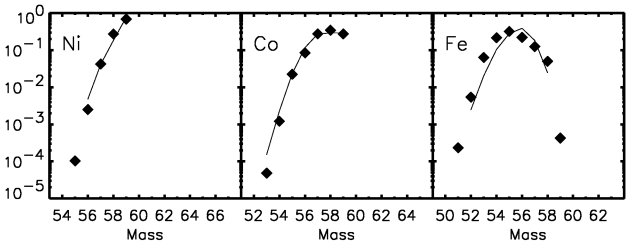

Fig. 5. Fractional yields from fragmentation of a 500 MeV/nucleon ^{60}Ni beam on a hydrogen target. The solid line represents predictions from the Silberberg and Tsao semi-empirical formulae. Data and predictions are separately normalized to the total yield for each element.

ited by uncertainties in the fragmentation cross sections used in the propagation models. Our relative yields for the daughter/stable ratios ^{49}Ti/(^{46}Ti+^{47}Ti+^{48}Ti) and ^{51}V/^{52}Cr appear qualitatively to account for some of the discrepancies between the cosmic-ray data and the propagation models.

We have also completed a preliminary analysis of fragmentation yields from a 500 MeV/nucleon ^{60}Ni beam on the hydrogen target. Figure 5 shows the relative yields of fragments from this beam, normalized as before to the total yield for each element. No prior data exists for ^{60}Ni fragmentation at these energies. The semi-empirical predictions (solid line) generally agree well in shape with our data, with some discrepancies for Fe isotopes. The mass-to-charge ratio of ^{56}Fe, in particular, is very close to that of the primary ^{60}Ni beam so cuts from the aluminum slits used to block the beam may affect the fit to the full velocity distribution. Further analysis of such isotopes will clarify whether the yields really show a significant deviation from the predictions.

The Fe-Ni group isotopes are important in cosmic rays for several reasons. These predominately primary species are good indicators of the nucleosynthetic composition of the source population. An apparent excess of ^{58}Fe material in the cosmic-ray source (Wiedenbeck et al., 2001a) may reflect an admixture of wind material from massive Wolf-Rayet stars which are enriched in the end products of core helium burning. The excess may also serve as a probe of the relative contribution of Type Ia supernovae to the source material. Radioactive decay primaries such as ^{59}Ni and ^{57}Co have been used to show that the time delay between nucleosynthesis and acceleration of the cosmic rays must be greater than $\sim 10^5$ years (Wiedenbeck et al., 1999). This result will be strengthened by the use of measured cross sections to determine the amount of ^{59}Ni produced by fragmentation of ^{60}Ni.

A proper normalization to the primary beam intensity must be completed before absolute cross sections can be obtained. For this preliminary report, we simply integrated the signal from the SEETRAM monitor for each setting. For the final result, a small positive bias must be subtracted from the SEETRAM signal and a careful calibration completed with data recorded for the purpose. Additionally, yields from the empty target runs must be subtracted to account for production in the target and the beam pipe structure. Comparison of the online trigger rates during runs in equivalent FRS settings suggests that production outside of the hydrogen accounts for $<15\%$ of the total fragment yield (and possibly much less). Improvements to the dead-time correction and fitting of gaps in the $\beta\gamma$ distributions as well as processing of data for the remaining energies will complete the analysis.

4 Summary

In summary, the interpretation of high-precision cosmic-ray abundance data from the ACE and Ulysses spacecraft is limited by uncertainties in the nuclear fragmentation cross sections, particularly in the sub-Fe ($20\leq Z\leq 25$) and Fe-Ni ($26\leq Z\leq 28$) groups. Isotopes in these groups address a wide range of important topics in cosmic-ray astrophysics, including the nature of the sources where nucleosynthesis occurs and the acceleration mechanisms that energize the particles produced by them.

New measurements of fragmentation cross sections from ^{56}Fe and ^{60}Ni have been made at energies relevant to galactic cosmic-ray propagation. Preliminary analysis of data taken at 500 MeV/nucleon indicate a qualitative agreement between the relative yields and semi-empirical models, and previous measurements of ^{56}Fe fragmentation. Some discrepancies with the formula predictions are noted, particularly for the rare and astrophysically important isotope ^{48}Ca.

A proper normalization of the relative yields to the primary beam intensity must be completed before absolute cross sections are obtained. Minor corrections to maximize resolution and an empty target subtraction are also underway. The analysis is proceeding steadily and it is hoped that final results can be released in the near future.

Acknowledgements. Participation in these measurements was supported at the California Institute of Technology and the Jet Propulsion Laboratory by NASA (under grant NAG5-6912). We gratefully acknowledge the assistance of the technical staff in the SIS and FRS groups at GSI.

References

Bowman, C.D., et al., *NIM A*, **320**, 336, 1992.
Connell, J.J. and Simpson, J.A., *Proc. 26th ICRC (Salt Lake City)*, **3**, 33-36, 1999.
Geissel, H., et al., *NIM B*, **70**, 286-297, 1992.
Golovanov, I.B., et al., *NIM A*, **381**, 15-22, 1996.
Niebur, S.M., et al., *Proc. 27th ICRC (Hamburg)*, 2001.
Pfützner, M., et al., *NIM B*, **86**, 213, 1994.
Silberberg, R., Tsao, C.H., and Barghouty, A.F., *ApJ*, **501**, 911, 1998.
Tsao, C.H., Silberberg, R., and Barghouty, A.F., *ApJ*, **501**, 920, 1998.
Webber, W.R., et al., *ApJ*, **508**, 949–959, 1998.
Wiedenbeck, M.E., et al., *ApJ*, **523**, L61-L64, 1999.
Wiedenbeck, M.E., et al., *Space Sci. Rev.*, 2001, in press.
Wiedenbeck, M.E., et al., *Proc. 27th ICRC (Hamburg)*, 2001.